Chemical Science

ROYAL SOCIETY OF CHEMISTRY

EDGE ARTICLE

View Article Online
View Journal | View Issue

Cite this: *Chem. Sci.*, 2021, **12**, 5224

All publication charges for this article have been paid for by the Royal Society of Chemistry

Received 24th January 2021
Accepted 23rd February 2021

DOI: 10.1039/d1sc00438g

rsc.li/chemical-science

Redox-induced reversible [2 + 2] cycloaddition of an etheno-fused diporphyrin†

Kazuya Miyagawa,[a] Ichiro Hisaki,[b] Norihito Fukui[a] and Hiroshi Shinokubo *[a]

3,5-Ethenoporphyrin is a π-extended porphyrin containing a fused ethene unit between the *meso*- and β-positions, exhibiting unique contribution of macrocyclic antiaromaticity. We have recently reported that its analogue, etheno-fused diporphyrin, underwent thermal [2 + 2] cycloaddition to furnish X-shaped cyclobutane-linked tetraporphyrins. Here we demonstrate that the cyclobutane-ring formation is dynamically redox-active. Namely, the tetraporphyrin underwent two-step four-electron oxidation to afford two etheno-fused diporphyrin dications. The reduction of the resulting dication regenerated the cyclobutane-linked tetraporphyrin. The dication was sufficiently stable to allow its isolation under ambient conditions. The structure of the dication has been confirmed by ^{1}H NMR spectroscopy and X-ray diffraction analysis. Importantly, the simultaneous double C–C bond cleavage in the cyclopropane ring in the tetraporphyrin is exceptional among dynamic redox (dyrex) systems to achieve large structural changes, thus offering new insights for the design of novel redox-active functional organic materials for electrochromic dyes, organic batteries, and organic memories.

Introduction

Porphyrins with extended π-conjugation networks exhibit numerous intriguing properties, such as near-infrared absorption, reversible redox activity, characteristic chemical reactivity, and high single-molecule conductance.[1] Such porphyrins have attracted considerable attention in various research fields including organic and supramolecular chemistry as well as materials science. 3,5-Ethenoporphyrin is an extraordinary π-extended porphyrin due to the coexistence of 18π-aromaticity and 20π-antiaromaticity in its macrocyclic conjugation (Fig. 1).[2,3] Consequently, 3,5-ethenoporphyrin exhibits a narrow HOMO–LUMO gap and high reactivity of the fused C–C double bond.

Recently, our research group envisaged the addition of another fused-porphyrin unit to the 3,5-ethenoporphyrin skeleton and attempted the synthesis of etheno-fused diporphyrin **1a** *via* the tandem double-cyclization of β,β-ethynylene-linked dibromodiporphyrin **2a** (Fig. 2).[4] Unexpectedly, we discovered the formation of cyclobutane-linked tetraporphyrins **3a** and **4a**. These two tetraporphyrins were formed through the thermal [2 + 2] cycloaddition reaction of *in situ*-generated **1a**. Due to orbital symmetry, the formation of the cyclobutane in **3a** *via* a [2 + 2] cycloaddition is thermally forbidden. Thus, the formation of **3a** and **4a** suggests the involvement of a thermally activated triplet state of **1a** in the thermal [2 + 2] cycloaddition reaction. Indeed, *syn*-tetramer **4a** isomerizes to *anti*-tetramer **3a** upon heating to 160 °C, which implies that the [2 + 2] cycloaddition of **1a** is thermally reversible.

We then decided to conduct further investigations into these cyclobutane-linked tetraporphyrins with a focus on their redox properties. Here, we disclose a reversible [2 + 2] cycloaddition through electron-transfer-induced cyclobutane ring-opening and -closure. This redox-induced reversible C–C-bond formation constitutes a dynamic redox (dyrex) system; such systems have been actively explored on account of their potential importance as electrochromic dyes, organic batteries, and organic memory devices.[5,6] Importantly, the simultaneous double C–C-bond formation/cleavage observed in the tetraporphyrin system is exceptional among reported dyrex systems.

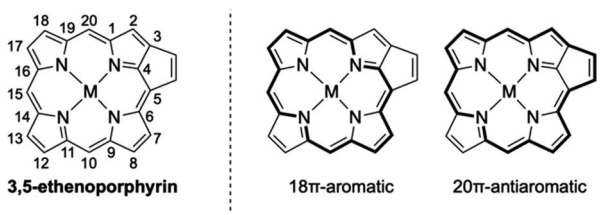

Fig. 1 Aromatic and anti-aromatic conjugation circuits of 3,5-ethenoporphyrin.

[a]*Department of Molecular and Macromolecular Chemistry, Graduate School of Engineering, Nagoya University, Furo-cho, Chikusa-ku, Nagoya 464-8603, Japan. E-mail: hshino@chembio.nagoya-u.ac.jp*

[b]*Graduate School of Engineering Science, Osaka University, 1-3 Machikaneyama, Toyonaka, Osaka 560-8531, Japan*

† Electronic supplementary information (ESI) available. CCDC 2055688 and 2055689. For ESI and crystallographic data in CIF or other electronic format see DOI: 10.1039/d1sc00438g

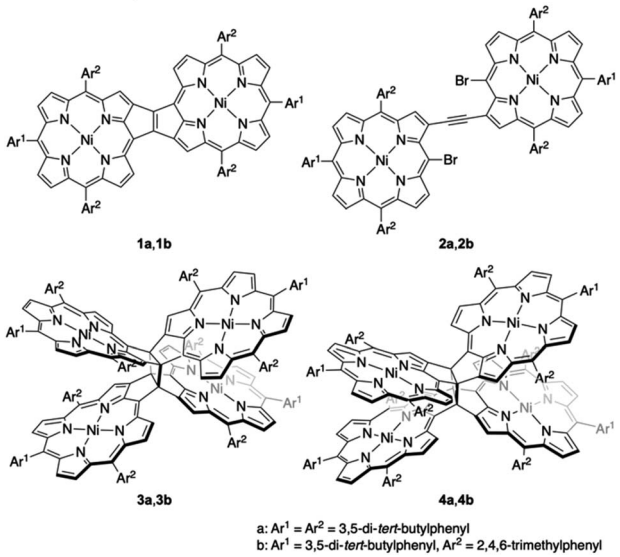

Fig. 2 Etheno-fused diporphyrin **1**, ethynylene-linked dibromodiporphyrin **2**, and cyclobutane-linked tetraporphyrins **3** and **4**.

Results and discussion

Synthesis and characterization of cyclobutane-linked tetraporphyrin

β,β-Ethynylene-linked dibromodiporphyrin **2b** was prepared according to a slightly modified literature procedure.[4,7] Precursor **2b** was subjected to a tandem double cyclization with $Ni(cod)_2$, which afforded *syn*-tetramer **4b** in 57% yield without the formation of *anti*-tetramer **3b** (Scheme 1). *anti*-Tetramer **3b** was not obtained even when the reaction temperature was increased to 60 °C. The selective formation of **4b** is due to the steric effect by bulky mesityl groups at the *meso*-positions. The structure of *syn*-tetramer **4b** was unambiguously determined by single-crystal X-ray diffraction analysis (Fig. 3).

Dyrex response of cyclobutane-linked tetraporphyrin

Cyclic voltammogram. The redox behavior of *syn*-tetramer **4b** was explored. The cyclic voltammogram of **4b** was measured in CH_2Cl_2 with tetrabutylammonium hexafluorophosphate as the supporting electrolyte (Fig. 4 and S20†). The ferrocene/ferrocenium couple (Fc/Fc^+) was used as an external reference. In the sweep from −0.60 V to 0.81 V, two peaks were observed at

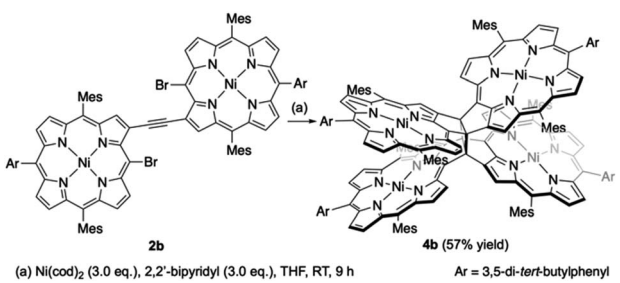

Scheme 1 Synthesis of *syn*-tetramer **4b**.

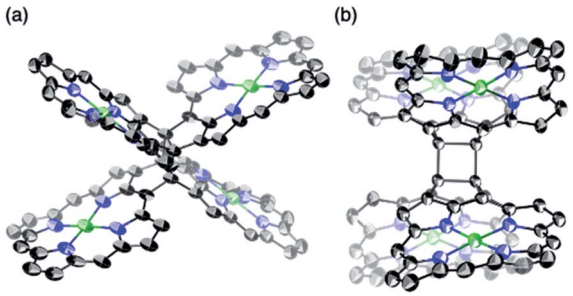

Fig. 3 Single-crystal X-ray crystal structure of *syn*-tetramer **4b**. (a) General and (b) side view. Thermal ellipsoids are drawn at 50% probability. Solvent molecules, peripheral aryl groups, and all hydrogen atoms are omitted for clarity.

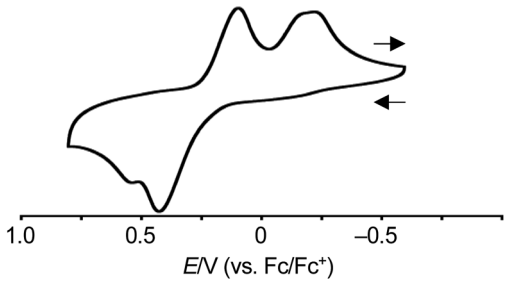

Fig. 4 Cyclic voltammogram of **4b**. Solvent: CH_2Cl_2; supporting electrolyte: 0.1 M $[Bu_4N][PF_6]$; working electrode: glassy carbon; counter electrode: Pt; reference electrode: $Ag/AgNO_3$; scan rate: 0.1 V s^{-1}.

0.43 and 0.56 V. These values are comparable to the first oxidation peak of porphyrin Ni(II) complexes (*ca.* 0.58 V).[8] In the case of porphyrin, the subsequent back-sweep generates a reduction wave at *ca.* 0.38 V. In contrast to porphyrin, *syn*-tetramer **4b** displayed reduction peaks at much lower values (0.10 and −0.29 V). The large displacement between the oxidation and reduction peaks implies the occurrence of dynamic structural changes.[5,6]

Oxidative titration. To obtain insight into the unique redox-response of *syn*-tetramer **4b**, we conducted an oxidative titration with tris(4-bromophenyl)aminium hexachloroantimonate (Magic Blue) in CH_2Cl_2 while measuring its absorption spectra, which demonstrated two-step spectral changes (Fig. 5). Clear isosbestic points were observed in both cases (Fig. S23†). The first change occurred after the consumption of *ca.* 2 equiv. of Magic Blue, resulting in the appearance of new peaks at 690 and 1274 nm. The further addition of Magic Blue (*ca.* 2 equiv.) resulted in the second change, which led to a slight blue shift of the absorption tail to *ca.* 1250 nm. Similar spectral changes were observed during spectroelectrochemical measurements from 0 to 1.2 V (Fig. S21†). Furthermore, the subsequent back-sweep to −0.5 V recovered the absorption peaks of *syn*-tetramer **4b**.

Isolation of the dication. The oxidation of *syn*-tetramer **4b** with 4 equiv. of Magic Blue in CH_2Cl_2 furnished etheno-fused diporphyrin dication $\mathbf{1b[SbCl_6]_2}$ in 89% yield (Scheme 2). The

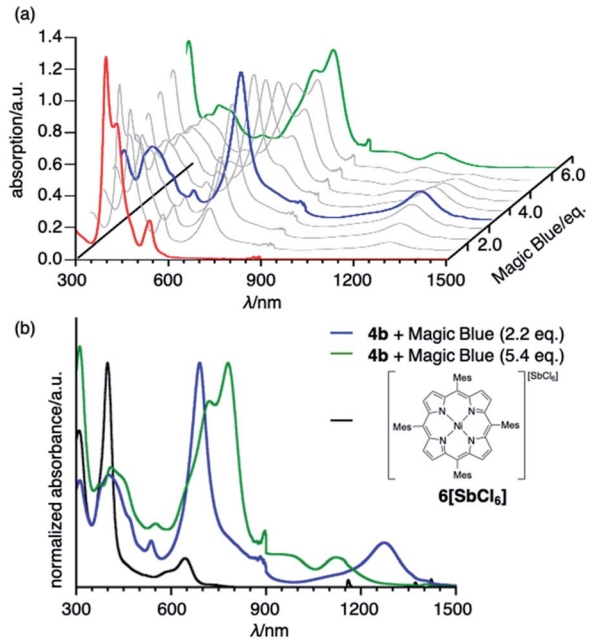

Fig. 5 (a) Oxidative titration of **4b** with Magic Blue. $[\mathbf{4b}]_0 = 3.0 \times 10^{-6}$ M^{-1}. (b) UV/vis/NIR absorption spectra of **4b** with 2.2 equiv. of Magic Blue, **4b** with 5.4 equiv. of Magic Blue, and porphyrin radical cation **6**[$SbCl_6$]. Solvent: CH_2Cl_2; λ: wavelength.

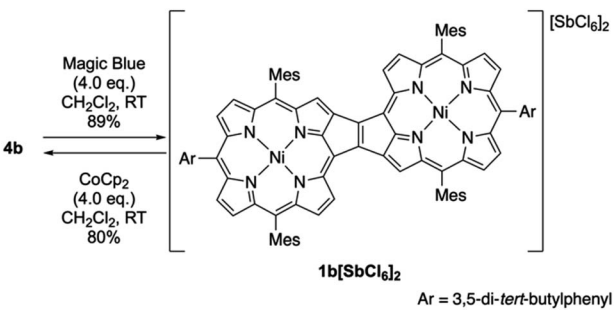

Scheme 2 Synthesis of etheno-fused diporphyrin dication **1b**[$SbCl_6$]$_2$.

reduction of **1b**[$SbCl_6$]$_2$ with an excess of cobaltocene recovered **4b** in 80% yield. While dication **1b**[$SbCl_6$]$_2$ is sufficiently stable under ambient conditions, repeated recrystallizations were required for its purification, given that **1b**[$SbCl_6$]$_2$ decomposes on silica gel. The ^{1}H NMR spectrum of **1b**[$SbCl_6$]$_2$ in $CDCl_3$ exhibited one singlet and six doublets (7.67–9.00 ppm) due to the main skeleton (Fig. 6). The calculated nucleus-independent chemical shift (NICS)[9] values of **1b**[$SbCl_6$]$_2$ nicely coincide with this observation (Fig. S27†). The presence of a distinct diatropic ring current in **1b**[$SbCl_6$]$_2$ can be rationalized by the removal of two electrons from the antiaromatic contribution of the etheno-fused diporphyrin core. Importantly, the signals due to the *ortho*-methyl groups of the mesityl substituents are observed as two singlet signals. Considering that **1b**[$SbCl_6$]$_2$ contains two magnetically inequivalent mesityl groups, this result indicates that each set of *ortho*-methyl groups is magnetically equivalent, supporting that **1b**[$SbCl_6$]$_2$ adopts a planar structure. The overall structure of **1b**[$SbCl_6$]$_2$ was determined based on single-crystal X-ray diffraction analysis, although the crystal data were not of sufficient quality to allow a detailed structural analysis (Fig. 7). Dication **1b**[$SbCl_6$]$_2$ adopts a completely planar structure with a mean plane deviation of 0.07 Å. The UV/vis/NIR absorption spectrum of **1b**[$SbCl_6$]$_2$ is in good agreement with that observed after the electrochemical oxidation of *syn*-tetramer **4b** (Fig. S21 and S22†).

Proposed dyrex-mechanism. The absorption spectrum after the addition of 2.2 equiv. of Magic Blue is clearly different from that of a porphyrin radical cation (Fig. 5b).[10] Considering that the inter-porphyrin interaction in *syn*-tetramer **4b** is essentially negligible due to the non-conjugative nature of the central cyclobutane unit, the initial change in absorption during the titration cannot be explained by the simple oxidation of **4b**. Furthermore, this absorption is in good agreement with a theoretical simulation of the radical cation of etheno-fused diporphyrin **1b**$^{\bullet}$ (Fig. S25†).

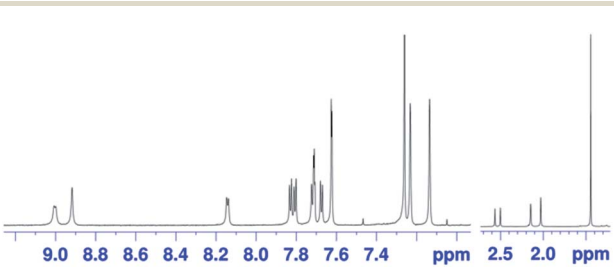

Fig. 6 ^{1}H NMR spectrum of **1b**[$SbCl_6$]$_2$ in $CDCl_3$ at 25 °C.

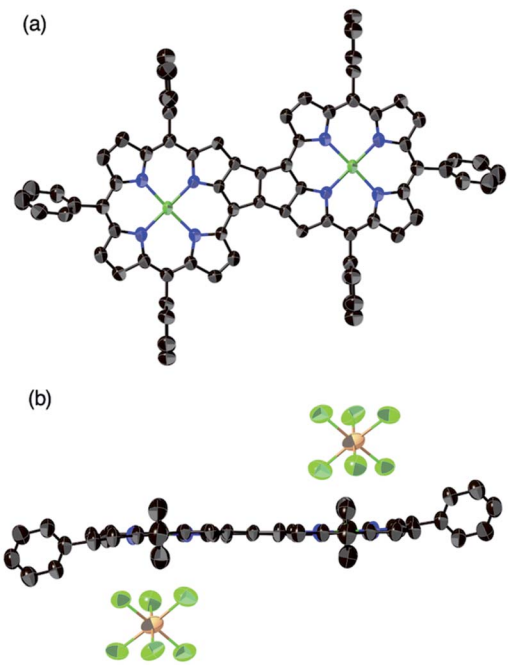

Fig. 7 Single-crystal X-ray diffraction structure of etheno-fused diporphyrin dication **1b**[$SbCl_6$]$_2$. (a) Top and (b) side view. Thermal ellipsoids are drawn at 50% probability. Solvent molecules, methyl groups, *tert*-butyl groups, and all hydrogen atoms are omitted for clarity.

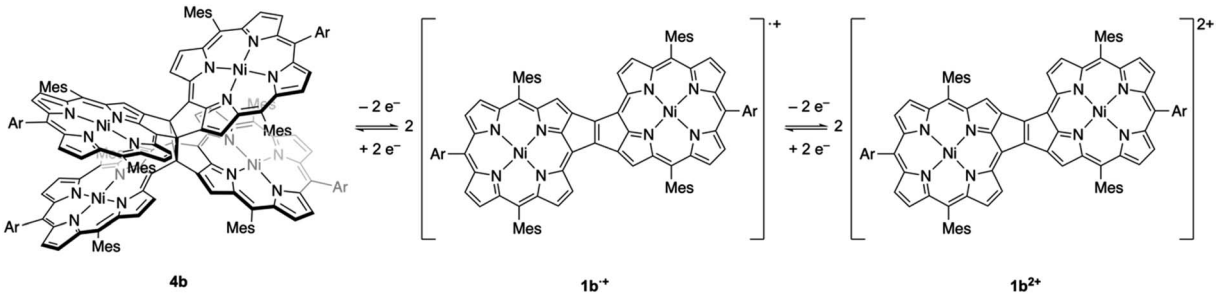

Scheme 3 Dyrex response of *syn*-tetramer **4b**.

Based on the results discussed above, we propose the following redox-response process for *syn*-tetramer **4b** (Scheme 3). The first two-electron oxidation of **4b** induces the cleavage of two C–C bonds at the central cyclobutane unit, affording two etheno-fused diporphyrin radical cations $\mathbf{1b}^{\bullet+}$. The subsequent oxidation of $\mathbf{1b}^{\bullet+}$ furnishes dication $\mathbf{1b}^{2+}$. The reverse reduction process begins with the one-electron reduction of dication $\mathbf{1b}^{2+}$. Our previous DFT calculations have predicted that the HOMO level of the etheno-fused diporphyrin is higher than that of a normal porphyrin due to the extended π-system and potential antiaromaticity.[4] Hence, the reduction potential of $\mathbf{1b}^{2+}$ can be expected to be much lower than the oxidation potential of **4b**, which would result in a large hysteresis in the cyclic voltammogram. Notably, we have also monitored a similar response during the electrochemical reduction of **4b** (Fig. S20†). However, the identification of the reduced species was unsuccessful owing to the instability of these intermediates.

Importantly, the redox response of **4b**, namely the reversible cycloreversion involving the cleavage of two C–C bonds, is exceptional among dyrex systems.[6,7] Quadricyclane, anthracene-dimer, and acridizinium dimer undergo double C–C bond cleavage upon electron-transfer, providing norbornadiene, anthracene, and acridizinium, respectively.[11–13] In these cases, however, the reverse C–C bond formation requires light-irradiation. The unique reactivity of the etheno-fused diporphyrin is attributed to the contribution of antiaromaticity in its macrocyclic conjugation. We believe that the current study offers a general insight that antiaromatic molecules[15] are a promising candidate for the design of novel redox-active functional organic materials including electrochromic dyes, organic batteries, and organic memory devices.

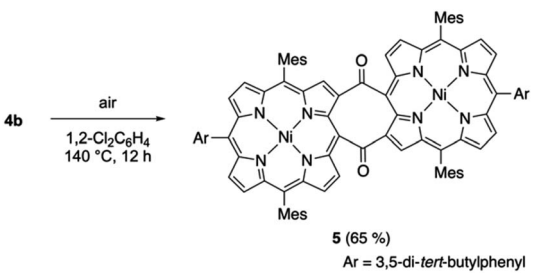

Scheme 4 Thermal conversion of *syn*-tetramer **4b** to **5** under aerobic conditions.

Thermal and photo-induced cycloreversion of cyclobutane-linked tetraporphyrin

We also examined the thermal cycloreversion of *syn*-tetramer **4b**, which was monitored using variable-temperature NMR and UV/vis absorption spectroscopy techniques. The ^{1}H NMR spectrum of **4b** in 1,2-dichlorobenzene-d_4 showed slight changes (up to 0.4 ppm) upon increasing the temperature from 20 °C to 120 °C (Fig. S18†). However, the absorption spectrum of **4b** in 1,2-dichlorobenzene displayed negligible changes upon heating (Fig. S19†). Consequently, the temperature-dependent change of the ^{1}H NMR chemical shifts can be attributed to the dynamic motion of the *meso*-aryl groups. Notably, heating the dichlorobenzene solution of **4b** to 140 °C afforded diketodiporphyrin **5** in 65% yield (Scheme 4). This result suggests the transient generation of etheno-fused diporphyrin **1b**, which is instantly oxidized to diketone **5**. A similar diketodiporphyrin was formed in our previous study with the corresponding zinc(II) complexes.[4] The excited state of nickel(II) porphyrins generally undergoes a rapid decay through the metal (d,d) state.[14] Consequently, the formation of diketodiporphyrin **5** implies that the thermally activated triplet state of *in situ*-generated etheno-fused diporphyrin **1b** reacted with triplet oxygen.

We also examined the effect of photo-irradiation on cycloreversion. A CH_2Cl_2 solution of **4b** was irradiated by a high-pressure mercury lamp equipped with a sharp cut filter (λ > 380 nm) (Fig. S24†). However, no detectable change was observed.

Conclusions

We have prepared X-shaped cyclobutane-linked tetraporphyrin **4b** and examined the thermal and redox-mediated cycloreversion of its cyclobutane-ring. Heating **4b** in 1,2-dichlorobenzene resulted in negligible changes in the ^{1}H NMR and UV/vis absorption spectra. Instead, *syn*-tetramer **4b** undergoes a two-step four-electron oxidation to afford etheno-fused diporphyrin dication $\mathbf{1b}^{2+}$. This redox-mediated cyclobutane-ring cycloreversion proceeds in a reversible manner and exhibits a large hysteresis in the cyclic voltammogram. Importantly, this process is accompanied by the cleavage of two C–C bonds, which is exceptional among dyrex systems. The current research highlights the unique reactivity of antiaromatic molecules and offers fundamental insights for the design of

novel redox-active functional organic materials including electrochromic dyes, organic batteries, and organic memory devices.

Author contributions

The manuscript was written through contributions of all authors. All authors have approved the final version of the manuscript. H. S. supervised the project and contributed to conceptualization, project administration, and writing (review & editing) the manuscript. K. M. carried out the synthesis and characterization. I. H. collected the X-ray data of **4b**. N. F. wrote the original draft.

Conflicts of interest

There are no conflicts to declare.

Acknowledgements

This work was supported by JSPS KAKENHI grant JP17H01190 and JP20H05863. H. S. gratefully acknowledges financial support from the Sumitomo Foundation. X-ray diffraction data of **4b** were collected at the BL40XU beamline of SPring-8 with approval of JASRI (proposal 2019B1134). The authors also thank Dr Nobuhiro Yasuda at SPring-8 (JASRI) for the collection of the X-ray diffraction data.

Notes and references

1 (*a*) H. L. Anderson, *Chem. Commun.*, 1999, 2323; (*b*) M. G. H. Vicente, L. Jaquinod and K. M. Smith, *Chem. Commun.*, 1999, 1771; (*c*) J. R. Reimers, N. S. Hush and M. J. Crossley, *J. Porphyrins Phthalocyanines*, 2002, **6**, 795; (*d*) S. Fox and R. W. Boyle, *Tetrahedron*, 2006, **62**, 10039; (*e*) N. Aratani, D. Kim and A. Osuka, *Chem.–Asian J.*, 2009, **4**, 1172; (*f*) C. Jiao and J. Wu, *Synlett*, 2012, 171; (*g*) J. P. Lewtak and D. T. Gryko, *Chem. Commun.*, 2012, **48**, 10069; (*h*) A. M. V. M. Pereira, S. Richeter, C. Jeandon, J.-P. Gisselbrecht, J. Wytko and R. Ruppert, *J. Porphyrins Phthalocyanines*, 2012, **16**, 464; (*i*) H. Mori, T. Tanaka and A. Osuka, *J. Mater. Chem. C*, 2013, **1**, 2500; (*j*) M. Grzybowski, K. Skonieczny, H. Butenschön and D. T. Gryko, *Angew. Chem., Int. Ed.*, 2013, **52**, 9900; (*k*) T. Tanaka and A. Osuka, *Chem. Soc. Rev.*, 2015, **44**, 943.

2 (*a*) A. Nakano, N. Aratani, H. Furuta and A. Osuka, *Chem. Commun.*, 2001, 1920; (*b*) A. K. Sahoo, S. Mori, H. Shinokubo and A. Osuka, *Angew. Chem., Int. Ed.*, 2006, **45**, 7972; (*c*) N. Fukui, H. Yorimitsu, J. M. Lim, D. Kim and A. Osuka, *Angew. Chem., Int. Ed.*, 2014, **53**, 4395; (*d*) N. Fukui, S. Arai, H. Shinokubo, H. Yorimitsu and A. Osuka, *Heterocycles*, 2015, **90**, 252.

3 (*a*) S. Fox and R. W. Boyle, *Chem. Commun.*, 2004, 1322; (*b*) D.-M. Shen, C. Liu and Q.-Y. Chen, *Chem. Commun.*, 2005, 4982; (*c*) D.-M. Shen, C. Liu and Q.-Y. Chen, *J. Org. Chem.*, 2006, **71**, 6508; (*d*) S. Hayashi, Y. Matsubara, S. Eu, H. Hayashi, T. Umeyama, Y. Matano and H. Imahori, *Chem. Lett.*, 2008, **37**, 846; (*e*) G. Bringmann, D. C. G. Götz, T. A. M. Gulder, T. H. Gehrke, T. Bruhn, T. Kupfer, K. Radacki, H. Braunschweig, A. Heckmann and C. Lambert, *J. Am. Chem. Soc.*, 2008, **130**, 17812; (*f*) T. D. Lash, B. E. Smith, M. J. Melquist and B. A. Godfrey, *J. Org. Chem.*, 2011, **76**, 5335; (*g*) A. M. V. M. Pereira, M. G. P. M. S. Neves, J. A. S. Cavaleiro, C. Jeandon, J.-P. Gisselbrecht, S. Choua and R. Ruppert, *Org. Lett.*, 2011, **13**, 4742; (*h*) T. Ishizuka, Y. Saegusa, Y. Shiota, K. Ohtake, K. Yoshizawa and T. Kojima, *Chem. Commun.*, 2013, **49**, 5939; (*i*) N. Fukui, W.-Y. Cha, S. Lee, S. Tokuji, D. Kim, H. Yorimitsu and A. Osuka, *Angew. Chem., Int. Ed.*, 2013, **52**, 9728; (*j*) K. Ota, T. Tanaka and A. Osuka, *Org. Lett.*, 2014, **16**, 2974; (*k*) N. Fukui, S.-K. Lee, K. Kato, D. Shimidzu, T. Tanaka, S. Lee, H. Yorimitsu, D. Kim and A. Osuka, *Chem. Sci.*, 2016, **7**, 4059.

4 T. Nagai, A. Takiguchi, M. Ueda, K. Oda, S. Hiroto and H. Shinokubo, *J. Am. Chem. Soc.*, 2018, **140**, 8392.

5 T. Suzuki, H. Tamaoki, J.-i. Nishida, H. Higuchi, T. Iwai, Y. Ishigaki, K. Hanada, R. Katoono, H. Kawai, K. Fujiwara and T. Fukushima, in *Organic Redox Systems: Synthesis, Properties, and Applications*, ed. T. Nishinaga, Wiley, Hoboken, 2015, ch. 2, pp. 13–37.

6 (*a*) H. Horner and S. Hünig, *J. Am. Chem. Soc.*, 1977, **99**, 6120; (*b*) J. Jubb, C. Floriani, A. Chiesi-Villa and C. Rizzoli, *J. Am. Chem. Soc.*, 1992, **114**, 6571; (*c*) T. Suzuki, J.-i. Nishida and T. Tsuji, *Angew. Chem., Int. Ed. Engl.*, 1997, **36**, 1329; (*d*) T. Muramatsu, A. Toyota, M. Kudou, Y. Ikegami and M. Watanabe, *J. Org. Chem.*, 1999, **64**, 7249; (*e*) S. Hünig, C. A. Briehn, P. Bäuerle and A. Emge, *Chem.–Eur. J.*, 2001, **7**, 2745; (*f*) S. Iwashita, E. Ohta, H. Higuchi, H. Kawai, K. Fujiwara, K. Ono, M. Takenaka and T. Suzuki, *Chem. Commun.*, 2004, 2076; (*g*) J.-i. Nishida, T. Miyagawa and Y. Yamashita, *Org. Lett.*, 2004, **6**, 2523; (*h*) J. K. Mahoney, V. Regnier, E. A. Romero, F. Molton, G. Royal, R. Jazzar, D. Martin and G. Bertrand, *Org. Chem. Front.*, 2018, **5**, 2073; (*i*) A. Gosset, L. Wilbraham, Š. N. Lachmanová, R. Sokolová, G. Dupeyre, F. Tuyèras, P. Ochsenbein, C. Perruchot, H.-P. J. de Rouville, H. Randriamahazaka, L. Pospíšil, I. Ciofini, M. Hromadová and P. P. Lainé, *J. Am. Chem. Soc.*, 2020, **142**, 5162.

7 K. Fujimoto and A. Osuka, *Chem.–Eur. J.*, 2018, **24**, 6530.

8 K. Fujimoto, H. Yorimitsu and A. Osuka, *Chem.–Eur. J.*, 2015, **21**, 11311.

9 Z. Chen, C. S. Wannere, C. Corminboeuf, R. Puchta and P. v. R. Schleyer, *Chem. Rev.*, 2005, **105**, 3842.

10 (*a*) A. Wolberg and J. Manassen, *J. Am. Chem. Soc.*, 1970, **92**, 2982; (*b*) D. Dolphin, T. Niem, R. H. Felton and I. Fujita, *J. Am. Chem. Soc.*, 1975, **97**, 5288.

11 (*a*) P. G. Gassman, R. Yamaguchi and G. F. Koser, *J. Org. Chem.*, 1978, **43**, 4392; (*b*) O. Brummel, D. Besold, T. Döpper, Y. Wu, S. Bochmann, F. Lazzari, F. Waidhas, U. Bauer, P. Bachmann, C. Papp, H.-P. Steinrück, A. Görling, J. Libuda and J. Bachmann, *ChemSusChem*, 2016, **9**, 1424.

12 (*a*) R. A. Barber, P. de Mayo, K. Okada and S. K. Wong, *J. Am. Chem. Soc.*, 1982, **104**, 4995; (*b*) J. M. Masnovi and J. K. Kochi, *J. Am. Chem. Soc.*, 1985, **107**, 6781.
13 H. Ihmels and J. Luo, *J. Photochem. Photobiol., A*, 2008, **200**, 3.
14 C. M. Drain, C. Kirmaier, C. J. Medforth, D. J. Nurco, K. M. Smith and D. Holten, *J. Phys. Chem.*, 1996, **100**, 11984.
15 (*a*) K. B. Wiberg, *Chem. Rev.*, 2001, **101**, 1317; (*b*) T. Nishinaga, T. Ohmae and M. Iyoda, *Symmetry*, 2010, **2**, 76; (*c*) H. Braunschweig and T. Kupfer, *Chem. Commun.*, 2011, **47**, 10903; (*d*) H. Hopf, *Angew. Chem., Int. Ed.*, 2013, **52**, 12224; (*e*) M. Rosenberg, C. Dahlstrand, K. Kilsa and H. Ottosson, *Chem. Rev.*, 2014, **114**, 5379; (*f*) C. K. Frederickson, B. D. Rose and M. M. Haley, *Acc. Chem. Res.*, 2017, **50**, 977; (*g*) Y. M. Sung, J. Oh, W.-Y. Cha, W. Kim, J. M. Lim, M.-C. Yoon and D. Kim, *Chem. Rev.*, 2017, **117**, 2257.